Ashok Ramasubramanian[1]
Department of Mechanical Engineering,
Union College,
Schenectady, NY 12308
e-mail: ramasuba@union.edu

Xavier Capaldi
Department of Physics,
Union College,
Schenectady, NY 12308

Sarah A. Bradner
Bioengineering Program,
Union College,
Schenectady, NY 12308

Lianna Gangi
Bioengineering Program,
Union College,
Schenectady, NY 12308

On the Biomechanics of Cardiac S-Looping in the Chick: Insights From Modeling and Perturbation Studies

Cardiac looping is an important embryonic developmental stage where the primitive heart tube (HT) twists into a configuration that more closely resembles the mature heart. Improper looping leads to congenital defects. Using the chick embryo as the experimental model, we study cardiac s-looping wherein the primitive ventricle, which lay superior to the atrium, now assumes its definitive position inferior to it. This process results in a heart loop that is no longer planar with the inflow and outflow tracts now lying in adjacent planes. We investigate the biomechanics of s-looping and use modeling to understand the nonlinear and time-variant morphogenetic shape changes. We developed physical and finite element models and validated the models using perturbation studies. The results from experiments and models show how force actuators such as bending of the embryonic dorsal wall (cervical flexure), rotation around the body axis (embryo torsion), and HT growth interact to produce the heart loop. Using model-based and experimental data, we present an improved hypothesis for early cardiac s-looping.
[DOI: 10.1115/1.4043077]

Keywords: heart development, cardiac looping, finite element modeling

1 Introduction

Cardiac looping results in the first easily visible breakage of left–right symmetry in the developing embryo. It is "a sequence of positional and morphological changes by which the originally straight and symmetric heart tube (HT) becomes transformed into an asymmetric heart loop" [1].

During looping, the HT is a simple tubular structure whose ends are referred to as the arterial and venous poles (Figs. 1 and 2(*a*)–2(*d*)). Blood enters through the latter and leaves through the former. Unidirectional blood flow is achieved in the absence of valves [2]. Looping can be divided into two sequential processes: c-looping and s-looping. The c-looping stage (Figs. 1(*a*) and 1(*b*)) results in the transformation of the initially straight heart tube into a twisted and curved tube [1,3].

The focus of this study is on early s-looping, which follows c-looping and results in two important positional changes: (1) the distance between cardiac inflow and outflow tracts is decreased and (2), the primitive ventricle migrates from its initial position cranial to the common atrium to its definitive position caudal to it (Figs. 1(*b*)–1(*d*) and 2(*a*)–2(*d*)). Although c-looping has been extensively studied from biochemical, genetic, and mechanical viewpoints, s-looping has received considerably less attention and its mechanics are not well understood.

At 22–23 days post conception (DPC, Carnegie stage 10), human embryos have their ventricles above the atria and looping begins. At 26–30 days DPC (CS 12), an s-shaped heart is formed and at 31–35 DPC (CS 14), the atria are above the ventricles [4]. In the chick embryo, the experimental model used here, these positional changes occur from about 48 to 56 h out of a total 21-day incubation period. The classic paper by Hamburger and Hamilton (HH) divides the incubation period of the chick into 46 stages [5]. The events considered in this study occur between HH stages 12–16.

Modeling is a powerful tool to understand the nonlinear and time variant shape changes that comprise cardiac looping. Several studies have used physical models to understand the complex multidimensional shape changes that occur during looping. The earliest instance that we could find is from 1928 where a physical model is used to demonstrate loop formation when the ends of a tube are brought together [6]. Physical models are also used to characterize the looping directionality and chirality of the s-loop [7,8]. In this study, we use physical models to gain basic insights and to aid in the development of computer models.

Finite element models have been used to uncover the mechanisms behind c-looping [3,9–11]. In this study, we present a comprehensive nonlinear finite element model for early cardiac s-looping. The model includes realistic heart geometry (including a multilayered cross section), experimentally validated material constants, and loads as suggested by experimental data. We use the model to develop an improved hypothesis for s-looping.

The s-loop (HH stage 15 or 16; Fig. 2(*d*); please also see Fig. 6(*d*) to understand the topology) may be described as follows [12]: "starting from the inflow tracts, which connect to the sinus venosus, the heart tube progresses in a cranial and ventral direction and at its peak is almost in direct contact with the distal end of the primitive head. Here, it turns around and follows a caudal dorsal course before turning cranialward again with the outflow tract again ending up near the head region where it is connected to the great arteries."

There are other significant morphogenetic shape changes that happen in the same time as cardiac s-looping: (1) the embryo undergoes rotation about its axis. Although eventually the whole embryo is rotated, during early s-looping, the rotation is confined to the cranial region (Figs. 5(*a*)–5(*d*)). Embryonic body torsion is a highly visible and yet often-ignored aspect of early embryo development. In this study, through experiments and models, we examine how head torsion and heart development influence each other (Sec. 3.1). (2) The dorsal body wall undergoes bending (segment between arrows in Fig. 3(*d*)) resulting in compressive forces being applied to the ends of the heart tube. This is cervical flexure. Some researchers argued that the looping heart pulled the dorsal body wall into the cervical flexure arc [13] while others posited

[1]Corresponding author.

Manuscript received July 13, 2018; final manuscript received March 4, 2019; published online March 27, 2019. Assoc. Editor: Jeffrey Ruberti.

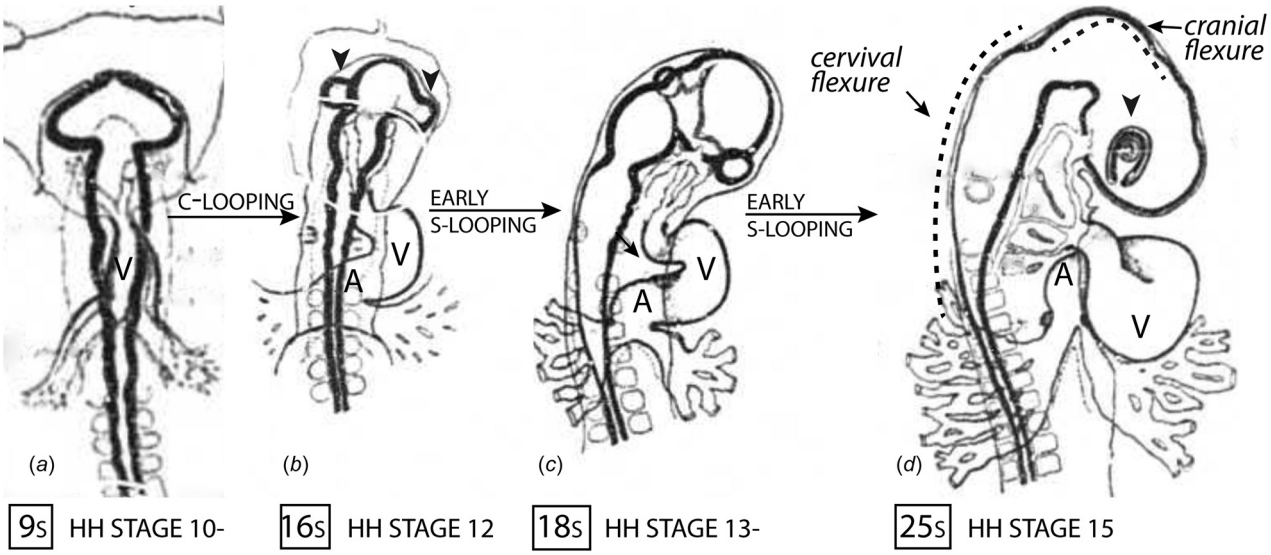

Fig. 1 An overview of cardiac looping, based on drawings from Ref. [15]. During c-looping ((*a*) and (*b*)), the initially straight HT is transformed into a c-shaped configuration. During early s-looping ((*b*)–(*d*)), the developmental stage considered here, the distance between the arterial and venous poles is shortened and the primitive ventricle migrates from its initial position cranial to the common atrium to its definitive position caudal to it. Note: (1) the formation of body flexures which happen at the same time as s-looping. Cranial flexure (which causes the axes of the forebrain and the hindbrain to form a right angle) and cervical flexure (broad curve on the dorsal body wall) are indicated in (*d*). (2) Head torsion—unrotated embryo has both eyes visible (indicated by arrowheads in (*b*)) while the rotated embryo has only eye visible (single arrowhead in (*d*)). Please note that the diagrams contain dorsal views. While a control embryo and its heart loop are shown here, improper loops formed due to perturbations are shown elsewhere in the paper. V = Ventricle, A = Atrium. Somite counts are indicated in boxes to the left of the stage labels.

that cervical flexure is an intrinsic process that caused heart looping.

Männer and colleagues showed that heart-removed embryos are able to form flexures in the total absence of cardiac forces [14]. As this is an important result, we repeated the experiments in this study using a different culture method and a different procedure to quantify curvature (Sec. 3.2).

In a previous study, we posited a hypothesis for early s-loop formation in which cervical flexure provides the driving force that buckles the heart tube and swaps the relative positions of the primitive atrium and ventricle [12]. But our new morphometric analyses indicate that embryos with small curvatures can have partial loops. Hence, some other factor also has a causal effect on looping. An obvious candidate is increase in length of the heart tube as investigated by other researchers [15,16]. In this study, we used a physical model to investigate if an increase in heart tube length can produce a topologically correct s-loop in the absence of flexure (Secs. 3.3 and 3.4). With the new experimental data and model-based analysis, we conclude this study by proposing an improved hypothesis for early s-looping (Sec. 4.4).

2 Methods

Experiments and models are described below. The sample size (n) and HH stages for the experimental data points are specified in Sec. 3.

2.1 Embryo Culture. Fertilized white leghorn chicken eggs (Charles River Labs) were incubated and embryos were harvested and staged according to the system of Ref. [5]. Embryos were cultured in vitro using the procedure described in Ref. [17]. The embryo develops with its ventral aspect in contact with the yolk and our culture method involves turning the embryo and culturing it ventral side up, to get better access to the heart. Therefore, our culture method provides ventral views of the heart up to stage 12 and ventrolateral (left lateral) views later as the embryo starts to rotate. Please note that this viewpoint swaps the left and right sides in images (the schematic in Fig. 1 contains dorsal views and has unswapped left and right sides). To better understand spatial relationships, we have used phrases such as "toward the observer" and "away from the observer"; the observer here is looking straight at a ventral view of the embryo or model.

The rotation mentioned above, however, is confined to the cranial portions of the embryo; the caudal portion of the embryo at the somite level is still unrotated in the stages considered here. Accordingly, the dorsal–ventral axis is noted as the horizontal direction for the heart region and separately, the left–right axis is indicated as the horizontal direction at the somite level (Fig. 2(*b*)).

2.2 Inhibition of Head Torsion. We used a fake eyelash of the sort used in cosmetics (Tmart, Inc.) to prevent head torsion in the developing embryo. The eyelash was threaded through the embryo at a location cranial to the developing heart (Fig. 2). This severely restricted the ability of the head to undergo further rotation. Using the eyelash as a handle, we were able to untwist the developing head and the developing heart. The heart so untwisted lost its nonplanar configuration and instead became a simple planar c-loop. This configuration was used to measure length of the heart tube (Sec. 2.5).

2.3 Heart Removal. Microscissors were inserted through a small hole in the splanchnopleure (SPL), a membrane that covers the heart [12]. The HT was severed at the most cranial section of the conotruncus and the most caudal section of the atrium. Heart-free embryos were then cultured for up to 10 h and their cervical flexure, cranial flexure, and head torsion were compared with those from control embryos. Heart regrowth occurred in many cases but we made sure via microdissection that the new proto tubes at the caudal and cranial ends never joined together.

2.4 Quantification of Cervical Flexure. Cervical flexure was quantified by measuring its radius of curvature and its length (Fig. 4(*a*)). The radius was measured by selecting 50–70 points, roughly equally spaced, and using these to fit a circle that

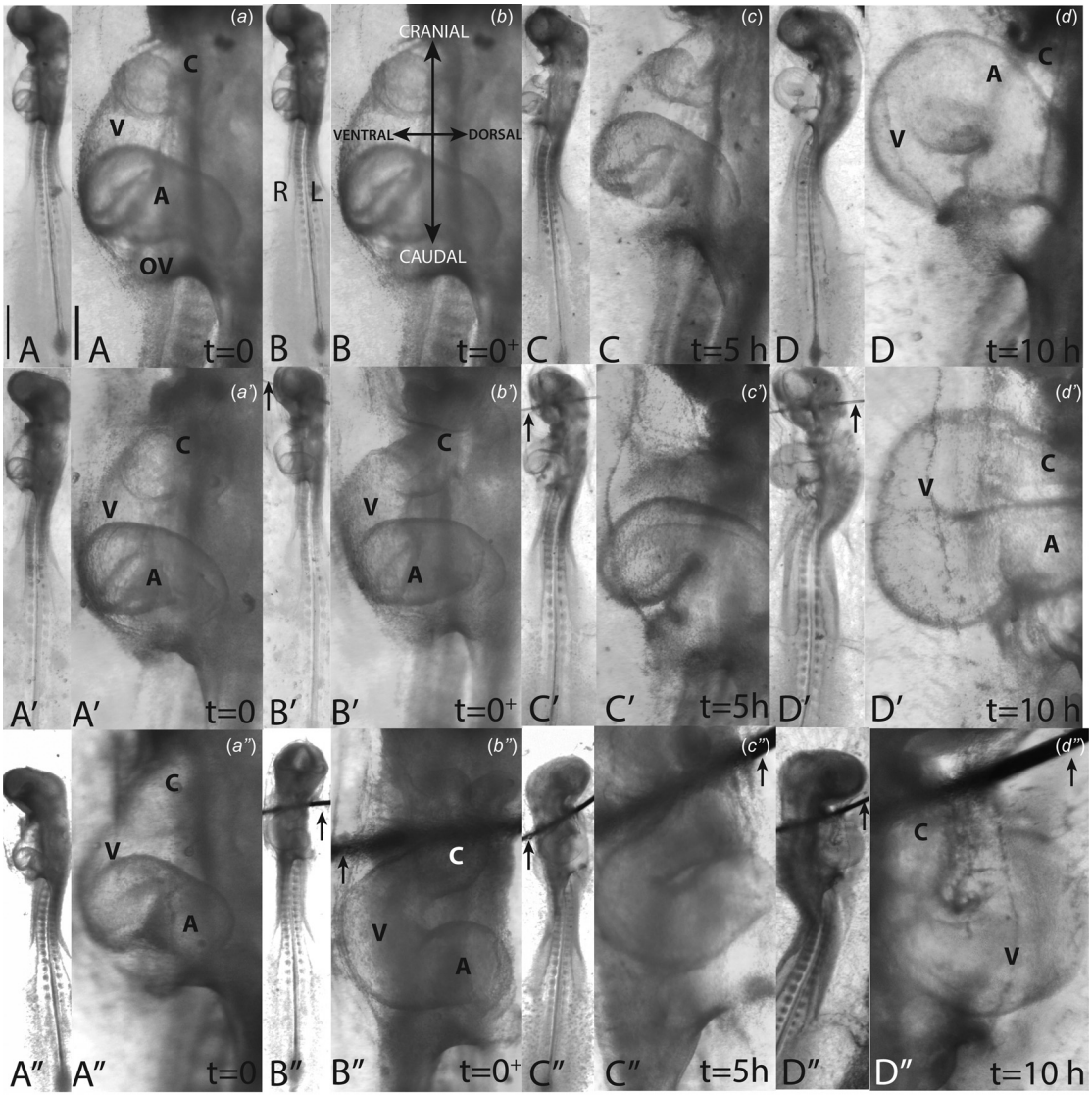

Fig. 2 Effect of impeding torsion on heart morphogenesis. For each time point, whole embryo (thin panels on the left) and isolated heart images are shown. ((*a*)–(*d*)) Control embryos. Note the formation of the normal cardiac s-loop with the ventricle moving inferior to the atrium (V = ventricle, A = atrium, C = conotruncus (outflow tract, arterial pole), and OV = omphalomesenteric veins, (inflow, venous pole)). When torsion is impaired by inserting an eyelash (indicated by arrows), two distinct topologies are observed. In a majority of the cases, a planar hairpin bend is observed ((*a*′)–(*d*′)). Although the arterial and venous poles of the heart tube can approach each other, no out-of-plane deformation is present (compare (*d*) with (*d*′)). In a few cases, a heart loop is formed on the *left* ((*a*″)–(*d*″)). Note that in both cases, there is considerable and easily visible untwisting of the heart at $t = 0^+$ when the eyelash is first inserted, showing clearly that removing body torsion untwists the heart tube and puts it in a planar configuration unsuitable for normal s-looping (transition from (*a*′) to (*b*′) and from (*a*″) to (*b*″)). Local embryo directions are shown in (*b*); Note that, as the embryo is partially rotated, the horizontal axis is the dorsal–ventral axis in the cranial portion, but it is the left–right axis in the caudal portion. L = left; R = right. Scale bar = 1 mm (whole embryo), 250 μm (heart close-ups).

minimized the squared error between the points and the circle fit. Points were selected using ImageJ and the least squares fit was done in Python/Numpy. A smaller radius in the fit circle corresponds to larger curvature. Cervical flexure is broadly defined as that portion of the embryonic dorsal wall between cranial and trunk flexures. We draw a straight line that is tangent to the optic vesicle and parallel to the head. The intersection of this line with the dorsal edge of the embryo locates the start of the cervical flexure segment (top arrow in Fig. 4(*a*)). The caudal end point of the cervical flexure segment is located at the point where the dorsal edge has an inflection point (bottom arrow in Fig. 4(*a*)).

Length of the cervical flexure segment was found using the same points by numerically evaluating a line integral. We started with 26 embryos in the control group and 22 in the heart removal group. Some measurements were discarded (especially at $t = 0$) for the following reasons: (1) for embryos whose dorsal walls were essentially straight, a large radius is attained that is sensitive to variations in the location of the points. We are trying to fit a circle to what is essentially a straight line and this is problematic. For this reason, radii larger than 5.6 mm were rejected from statistical analysis. This occurred mostly at $t = 0$ when cervical flexure is just starting to form, but also at $t = 10$ h for three embryos in the heart-removal group because flexures of these embryos retained straight line segments. (2) In many of the above cases, it is still possible to measure the length of the cervical flexure segment. However, in a few cases, length measurements were also

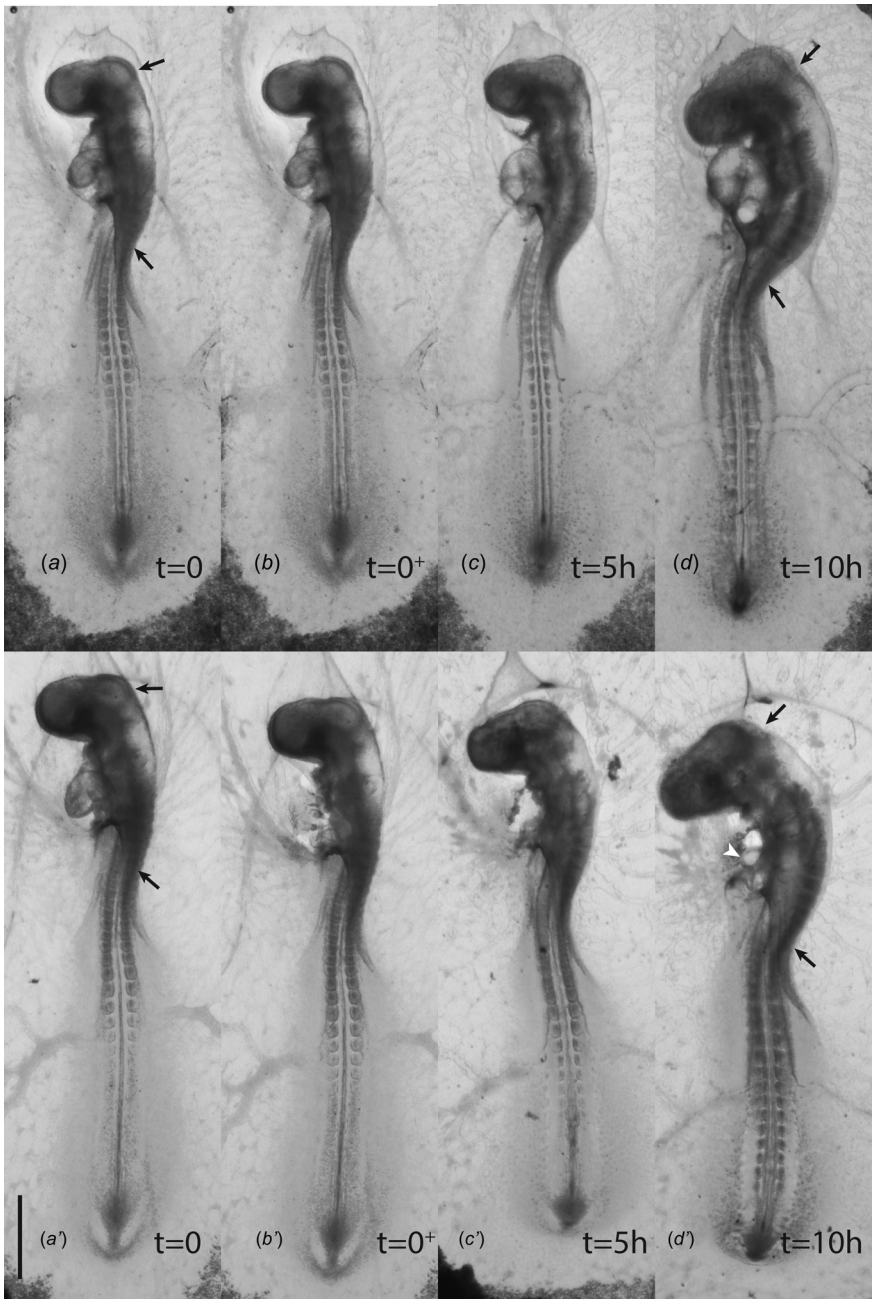

Fig. 3 Effect of heart removal on the formation of cervical flexure. ((*a*)–(*d*)) Control embryo at time points indicated. Cervical flexure (section between black arrows in (*a*)–(*d*)) increases. ((*a′*)–(*d′*)) Embryo at a similar starting stage in which the heart has been removed at $t = 0^+$ ((*b′*)). Cervical flexure (section between black arrows in (*a′*)–(*d′*)) can still occur without the aid of the looping heart. Most heart-free embryos regrew primitive tubular structures resembling the heart. Regrowth was most prominent in the caudal end of the heart tube remnant (white arrowhead in (*d′*)). Scale bar = 1 mm.

discarded at $t = 0$ because the start and end of the cervical flexure segment could not be accurately determined. Please note that all significant conclusions are made based on data from $t = 10$ h when more measurements are available. n values are explicitly stated for each case in Sec. 3 (Sec. 3.2.1).

2.5 Heart Tube Length Measurements. Due to the nonplanar nature of the s-loop, measuring heart tube lengths during s-looping is difficult. Even the preloop has the primary heart segments, the conotruncus, ventricle, and atrium in different frontal planes (Fig. 2(*a*)). Hence, we used the embryos where heart rotation was removed (Sec. 2.2). This perturbation forces the heart segments to be in approximately the same plane (Figs. 2(*b′*)–2(*d′*)). The outer curvature was traced in ImageJ to measure lengths at $t = 0$ and $t = 10$ h. We measured the length from the caudal endpoint of the conus to the omphalomesenteric veins (OVs). It is possible that the inhibition of rotation has an effect on length. This effect, if present, is not quantifiable with our methods. Measurements were also restricted to those embryos with loops that were mostly planar after rotation was removed. There are additional challenges (please see Sec. 4.1 for a discussion).

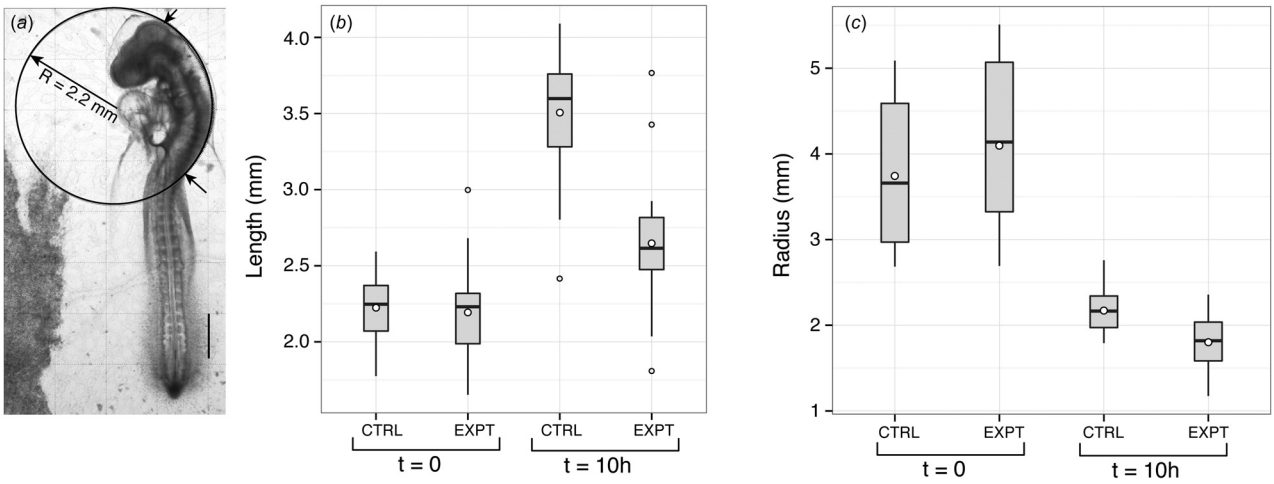

Fig. 4 Length and radius of cervical flexure. (*a*) Illustration of our methodology (Sec. 2.4). Least squares best-fit circle is shown. Arrows indicate the start and end of cervical flexure segment. (*b*) Box plot of cervical flexure lengths (measured using line integrals) at $t = 0$ and $t = 10$ h for control (CTRL) and heart-free cultures (EXPT). The box contains the middle 50% of the data and the whiskers contain the top and bottom 25%. Outliers are shown as open circles. The horizontal line and the circle within the boxes indicate the median and the mean, respectively. (*c*) Box plots of cervical flexure radii at $t = 0$ and $t = 10$ h. Scale bar = 1 mm.

2.6 Physical Model. As in previous studies [7,16], we used a physical model to study the salient morphological changes that occur during cardiac looping. To visualize how head torsion and cervical flexure influence looping, a solid rubber tube was used to model the looping heart. The tube was attached at two points to a flexible "goose neck" rod. The rod denotes the embryonic head and neck and, matching experiment, is much stiffer than the rubber tube (heart) [18]. The tube and the rod lie against a white board, which denotes the structures at the dorsal side of the unlooped heart (Fig. 6). The top of the rubber tube is rotated by 90 deg prior to clamping to the rod. The bottom end of the tube is clamped without any rotation. This setup results in torsion of the heart tube as observed in experiments (Figs. 6(*a*) and 6(*b*) for model and Figs. 2(*a*)–2(*c*) for experiment). At this point, cervical flexure is simulated by bending the goose neck rod to match the curvature observed in experiments (Figs. 6(*b*)–6(*d*) for model and Figs. 2(*b*)–2(*d*) for experiment). Note that bending of the metal rod is not uniform along its length ((*b*)–(*d*) and (*b*′)–(*d*′) in Fig. 6) and more bending is applied to the cranial portion resulting in a question-mark ("?") shaped configuration as in the experiment (Fig. 2(*d*)). Please note some important differences between the physical model setup and the experiment—(1) the heart and head/neck are modeled as slender tubes, whereas they are not so in the experiment, (2) the increase in the length of the cervical flexure arc is not captured in the model, and (3) the model has significantly higher gravitational loads. In spite of these differences, as in earlier studies, the model provides an opportunity to test and visualize interplay between heart looping, head torsion, and cervical flexure.

In a separate model, we used concentric tubes to simulate growth in the heart tube (Figs. 6(*a*″)–6(*d*″)). A portion of a solid tube is inserted into a hollow tube (Fig. 6(*a*″)) and growth is simulated by gradually pulling the solid tube from the hollow tube (Figs. 6(*b*″)–6(*d*″)). The growth ratio, λ_g, is the ratio of the new total length to the old total length. The outer diameter of the solid tube matches the inner diameter of the hollow tube.

2.7 Finite Element Modeling. We developed finite element models to study looping under both normal and perturbed conditions. Based on experimental data, we used a simple yet realistic initial geometry that consisted of a c-shaped heart tube that has completed c-looping, but has not yet started s-looping (Fig. 7(*a*)). Similar to experiment, the model has a nonhomogeneous cross section where a thin outer layer of myocardium envelopes a much thicker layer of cardiac jelly, the extracellular matrix (inset in Fig. 7(*a*)). Both materials are assumed by hyperelastic with the following moduli: 11.05 Pa for the myocardium and 3.2 Pa for cardiac jelly, as determined experimentally [19].

Two separate loads are applied: (1) head torsion is simulated by applying a 90 deg rotation at the top surface of the conotruncus (Fig. 7(*a*)) and (2) body flexure, which results in the arterial and venous poles coming toward each other, is simulated by applying an upward displacement to the venous pole while holding the arterial pole fixed. Torsion and flexion loads are applied sequentially (torsion first). This is because even though torsion and flexion are coupled processes, they have distinct roles in effecting s-looping. Our hypothesis posits that torsion is necessary for displacing the arterial pole of the heart tube into a different frontal plane and flexion is necessary to bring the two poles together.

As looping proceeds, in simulation as in the experiment, the arterial and venous poles slide past each other. This contact is modeled as a frictionless tangential surface interaction. The geometry was created in SOLIDWORKS 2017 (Dassault Systemes) and exported as a ParaSolid Transmit file. A quadratic (element order), tetrahedral (element shape), contiguous mesh was generated in PATRAN 2011 (MSC software). A contiguous mesh is one in which the inner surface of the myocardial tube matches the outer surface of the cardiac jelly. This eliminates the need to use additional surface to surface binding constraints during simulation. Nonlinear finite element simulation was performed using ABAQUS/Standard (Dassault Systemes, version 6.13). Nonlinear material properties are specified using subroutine UMAT.

2.8 Statistical Analysis. Two-tailed t-tests were used to compare the population means of numerical measurements. All statistical analysis was done in *R* (version 3.2.2) using the t-test function. This function does not assume equal variances between groups, which makes the results more robust. All numerical data are presented as mean ± standard deviation. Box plots were generated using *R* package ggplot2. A p value of 0.05 was used to test for statistically significant differences.

3 Results

3.1 Effect of Inhibiting Head Torsion. To study the influence of head rotation on cardiac looping, we inserted an eyelash

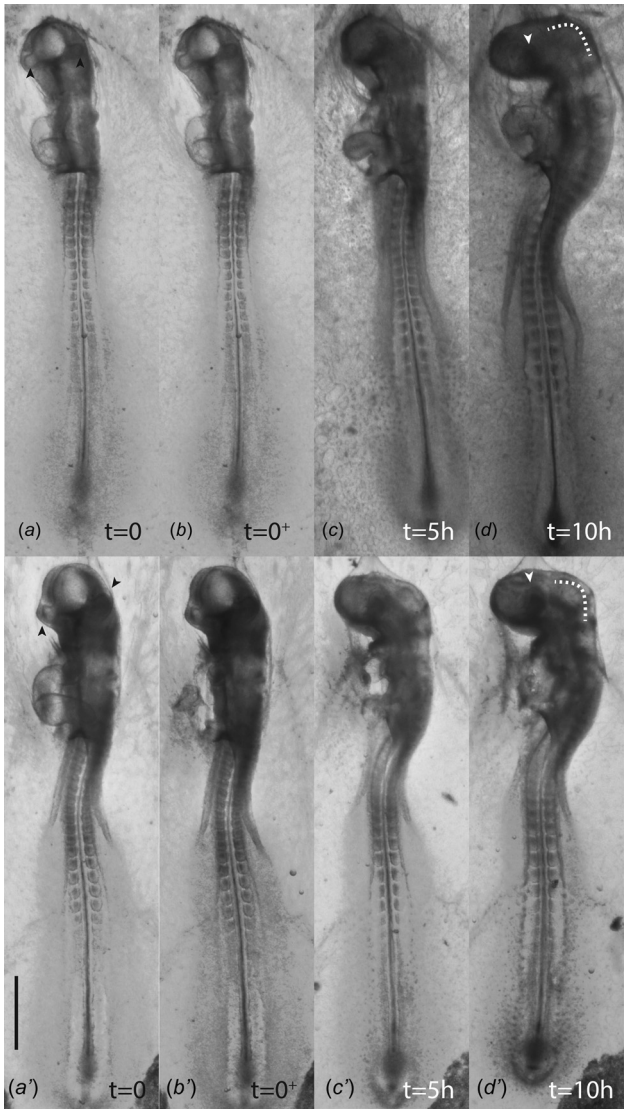

Fig. 5 Heart removal does not inhibit head rotation and cranial flexure. ((*a*)–(*d*)) control embryo, ((*a*′)–(*d*′)) heart-removed embryo. The angle between the forebrain the hindbrain eventually becomes 90 deg indicating normal cranial flexure (shown by dotted white lines in (*d*) and (*d*′)), whereas both eyes are visible initially (arrowheads in (*a*), (*a*′)), by $t = 10$ h, head rotation is complete and only one eye is visible (single arrowhead in (*d*), (*d*′)). Scale bar = 1 mm.

through the developing head or neck and untwisted the embryo ($t = 0$ is just before eyelash insertion and $t = 0^+$ is immediately following). This had the effect of removing or reducing any existing body torsion and impeding further torsion. Eyelashes were inserted in 25 stage 13 or 14 embryos where s-looping is just starting, i.e., the ventricle is still superior to the atrium and the poles are farther apart than they would be in a completed loop. The effects of unrotation were observed at $t = 0$ (before untwist), $t = 0^+$ (immediately after untwist), $t = 5$ h, and $t = 10$ h.

Twenty three embryos (92%) had a noticeable untwist at $t = 0^+$, i.e., the conotruncus and the primitive ventricle, which lie more backward (i.e., away from the observer) compared to the atrium, are now brought forward (i.e., toward the observer) due to the untwist in the cranial region (transitions from Figs. 2(*a*′) to 2(*b*′) and from Figs. 2(*a*″) to 2(*b*″); compare with control embryo in Fig. 2(*a*)). In other words, the out-of-plane character of the normal preloop is lost and the untwisted embryos have the conotruncus, ventricle, and atrium all located more or less in the same plane (Figs. 2(*b*′) and 2(*b*″)).

The embryo responds to this improper preloop in two distinct ways. In the majority of cases (17/25, 68%), development proceeds with the improper in-plane preloop, resulting in a planar configuration where the conotruncus and the atrium come into contact (Fig. 2(*d*′)). We refer to this as the "hairpin bend" configuration. This is in contrast to control embryos where the normal preloop progresses with the conotruncus slipping behind the atrium to complete the s-loop (Fig. 2(*d*)).[2] In a minority of the cases (5/25, 20%), a heart loop at varying levels of completion forms on the left side of the embryo at $t = 10$ h (Figs. 2(*a*″)–2(*d*″)). Precise quantitative analysis of the extent of these anomalous topologies was not carried out because of the small sample size ($n = 5$). One (4%) had a partially completed s-loop on the right and two of the embryos (2/25, 8%) died or were nearly dead at $t = 10$ h.

3.2 Effect of Heart Removal

3.2.1 Effect on Cervical Flexure. Hearts were removed from embryos where rotation is complete in the cranial region and the angle between the forebrain and hindbrain axes is approximately 90 deg; cervical flexure is just starting to form. This corresponds to about HH stage 14. Images were acquired at $t = 0$ (just before heart removal), $t = 0^+$ (just after heart removal), and $t = 10$ h to observe development of cervical flexure (Fig. 3). Numerical data are summarized in Fig. 4. Length and radius of the cervical flexure arc were measured (Sec. 2.4). Please note that a smaller radius means larger curvature.

Length of the cervical arc increased robustly in control embryos: 2.22 ± 0.24 mm at $t = 0$ ($n = 24$) to 3.51 ± 0.41 at $t = 10$ ($n = 26$), but the increase in length for heart-removed embryos was smaller: 2.19 ± 0.32 mm at $t = 0$ ($n = 22$) to 2.65 ± 0.42, at $t = 10$ h ($n = 22$). The difference in lengths at $t = 10$ h between control and heart removal groups was statistically significant ($p \ll 0.01$). In other words, there is overwhelming evidence to suggest that at $t = 10$ h, the control lengths are on average larger than the experimental lengths. As expected, there was no statistically significant difference in length ($p = 0.72$) or curvature ($p = 0.29$) at $t = 0$ between the two groups.

Curvature increased robustly in both control and heart removal groups. However, due to the differing rates of length increase, the curvature of heart-removed embryos was bigger (i.e., the radius was smaller) at $t = 10$ h: for control embryos, the radius decreased from 3.74 ± 0.86 mm at $t = 0$ ($n = 21$) to 2.17 ± 0.25 mm at $t = 10$ h ($n = 26$), while for heart-removed embryos, the radius decreased from 4.10 ± 0.96 mm at $t = 0$ ($n = 13$) to 1.80 ± 0.32 mm at $t = 10$ h ($n = 19$). Three embryos in the experimental group (14%) retained straight segments in the cervical flexure during development and their flexures did form a perfect circular arc. Curvature was not measured for these embryos (Sec. 2.4).

The difference in curvature at $t = 10$ h between control and heart removal groups was again found to be statistically significant ($p \ll 0.01$), but this statistical significance vanished when the curvatures were normalized with lengths. The mean of the radii divided by the lengths at $t = 10$ h is quite similar: 0.63 and 0.68 for controls and heart-removed groups, respectively. This small difference is not statistically significant ($p = 0.2$). Hence, when the curvature is normalized with length, there is no statistical difference between flexure formation in control and heart-free embryos.

A few embryos did experience a small decrease in curvature immediately following heart removal, suggesting relaxation after loss of tensile forces applied by the heart; however, in the entire sample, there was no statistical difference in curvature between $t = 0$ and $t = 0^+$ ($p = 0.77$). Interestingly, we found cardiac tube regrowth at both the severed ends. Regrowth at the caudal end

[2]Shapes can be slightly different due to natural biological variability; a different example of the hair insertion experiment is shown in Fig. 8 along with our computer model.

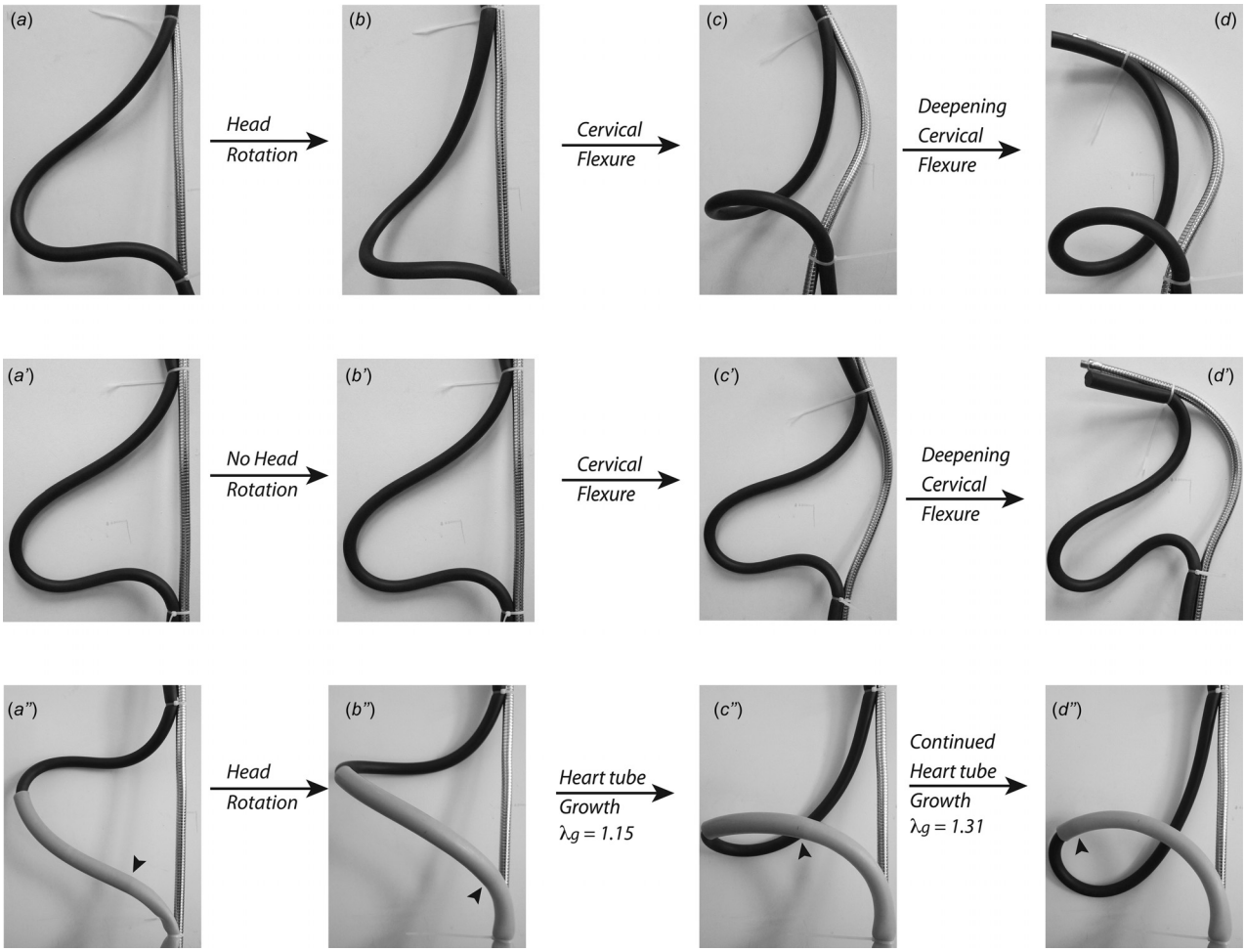

Fig. 6 A physical model for the s-looping heart tube. The "goose neck" metal rod denotes the head and the rubber tube (black) denotes the heart. The tube and the rod lie against a white board, which denotes the structures at the dorsal side of the heart. (*a*)–(*d*) The baseline model. Head rotation (implemented by rotating the top end of the tube 90 deg and clamping) ensures that the cranial part of the tube is displaced backward compared to the caudal part ((*a*) → (*b*)). When this necessary step is completed, bending of the metal rod, which corresponds to cervical flexure, can twist the tube into a loop ((*b*) → (*c*) → (*d*)). In the absence of the crucial rotation step, no loop is formed; instead a hairpin bend results ((*a*′)–(*d*′)) as in experiment (compare topology in (*d*′) with Fig. 2(*d*′)). While rotation seems to be necessary for looping, the model shows that a basic loop can form in the absence of cervical flexure when the tube is allowed to elongate ((*a*″)–(*d*″)). A solid tube extracted from a hollow tube ((*a*″)) simulates growth. To start with, rotation is applied as in the baseline model ((*a*″) → (*b*″)). At this point, the rubber tube is allowed to "grow" by gradually pulling out the segment of the solid tube that is within the hollow tube. In (*a*″)–(*d*″), arrowheads show the extent of the solid tube that is inside the hollow tube.

was especially significant and by $t = 10$ h a primitive tubular stump was visible in most of the embryos (white arrowhead in Fig. 3(*d*′)). Many of these regrown heart tubes were also pulsating. In embryos where regrowth was so significant that the rudiments at arterial and venous poles threatened to come into to contact, we cut again to ensure that no forces were transmitted from the heart.

3.2.2 Effect on Head Torsion and Cranial Flexure. Hearts were removed from 11 stage 12/13 embryos whose cranial flexure (formation of the 90 deg bend between the axes of the forebrain and the hindbrain—Fig. 5(*d*)) and head rotation were just starting or had not yet started. Most of them (9/11, 82%) showed good progress in both flexure and rotation (Fig. 5). Two embryos (18%) only had slight improvement in flexure and rotation and these two were among the youngest in the experimental group. Overall, we found a correlation between the morphological progression in cranial flexure and head rotation.

3.3 Heart Tube Length Changes During Early S-Looping. Length measurements were performed in embryos ($n = 7$) where the s-loop was rendered almost perfectly planar by using the hair insertion procedure outlined in Sec. 2.2. Lengths at $t = 0$ (approximately HH 13–14) and $t = 10$ h were 1.32 ± 0.15 mm and 1.97 ± 0.26 mm, respectively. This gives a growth stretch ratio of $\lambda_g = 1.49$.

3.4 Physical and Computational Models. Physical and computer models were used to study the mechanical forces influencing s-looping. In the models without perturbations, a combination of head rotation and cervical flexure ensures that a loop, with the same topology as in experiment, is able to form (compare Figs. 6(*a*)–6(*d*) and 7(*a*)–7(*d*) with Figs. 2(*a*)–2(*d*)). Head rotation provides the looping directionality while flexure provides the driving force. When rotation is removed, similar to experiment, a hairpin bend is formed in both models where all the primitive heart segments lie in the same plane (compare Figs. 6(*d*′) and 8(*d*) with Fig. 2(*d*′)). Similar to the experiment, the length and radius of curvature of the cervical flexure segment were computed for the physical model (Sec. 2.4). The ratio, radius divided by length, was 0.65 for an initial loop (Fig. 6(*c*)) and 0.41 for the full loop (Fig. 6(*d*)).

We used concentric tubes to simulate growth in the physical model. Figures 6(*a″*)–6(*d″*) show that while rotation is still needed to influence directionality, the driving force behind loop formation can also come from heart tube growth. The initial length between the tube's attachment points in Fig. 6(*a″*) is about the same as that in Fig. 6(*a*); pulling out the segment of the solid tube that is inside the hollow tube allows us to simulate growth. A basic loop is able to form at 15% growth ($\lambda_g = 1.15$). When growth is about 30% ($\lambda_g = 1.31$), one is able to obtain a loop that is topologically indistinguishable from the one that is formed due to flexure (compare loops in Figs. 6(*d*) and 6(*d″*)).

4 Discussion

Cardiac looping is an important phase in heart development. It can be divided into two sequential processes: c-looping and s-looping (Fig. 1). C-looping is the first phase of looping in which the initially symmetric HT bends ventrally and simultaneously twists to the right [1,9,20]. It represents the first visible breakage of left–right symmetry in the embryo and has been studied in detail from biochemical, genetic, and mechanical standpoints (please see Ref. [3] for a review).

C-looping in the chick is comprised of ventral bending of the HT, which is driven by actin polymerization-induced cell-shape changes [21] and dextral rotation of the HT, which is driven by asymmetric growth in the omphalomesenteric veins and downward pressure applied by the splanchnopleure, a membrane on the ventral side of the HT. The dorsal mesocardium (DM), a strip of tissue at the dorsal midline of the HT acts a hinge about which rotation occurs [9]. The DM is also implicated in the autonomous regulation of looping under both control and perturbation conditions [10]. Recent evidence indicates a significant role for the DM in heart looping in mouse [22] and quail [23]. In the chick, the DM ruptures during c-looping and is not active during s-looping [1,9]. Improper c-looping can lead to laterality defects ([24] and references therein). And improper looping, along with other cardiac malformations, is linked to spontaneous abortions [25].

S-looping, which follows c-looping, has received relatively little attention. In this study, we focus on early s-looping where the ventricle moves to its final position caudal to the atrium. In a previous study, we investigated if some players in c-looping (cardiac jelly inflation and pressure from the splanchnopleure) played any role during early s-looping. We concluded that the c-looped heart has no intrinsic ability to form an s-loop and that external factors such as cervical flexure and head torsion are necessary.

In this paper, we extend our previous results and take a closer look at the interplay between shape changes in the heart (s-looping) and those at the head and neck regions (head torsion, cranial flexure, and cervical flexure). In particular, our results shed light on the largely ignored role of head torsion on s-looping. We also confirmed the results of previous studies relating cervical flexure and looping and quantified the role of heart tube length increase. A combination of experimental data, physical models, and computer models is used to arrive at an improved hypothesis for early s-looping.

4.1 Remarks on Link Between Cardiac Looping and Heart Tube Length. Patten provides a summary of the increase in heart tube length during looping [15]. The data in this classic paper are compiled neatly in Ref. [16]. During early s-looping, the HT length increases from about 1.5 mm prior to s-looping (HH stage 13+) to about 2.1 mm at its completion (HH stage 15). That is an elongation of 40% (growth stretch ratio $\lambda_g = 1.40$). Two striking features can be discerned from Patten's data: (1) even though the HT increases in length all the way from HH 10 (pre c-loop) to HH 21+ (well beyond s-looping), the *rate* of increase is maximized between stages 13 and 16, which includes early s-looping. (2) During early s-looping, the pericardial cavity length remains essentially flat. There is thus clear evidence that during early s-looping, the HT increases dramatically in length, while the length of the pericardial cavity enclosing it does not.

To our knowledge, no other recent study has attempted to quantify the increase in heart tube length during looping; it is quite challenging to do so. The attachments of the heart tube to the body of the embryo at its arterial and venous poles are not easy to discern. This problem is particularly acute at the caudal end of the tube where the primitive atrial segment connects to a pair of omphalomesenteric veins (OVs, Fig. 2(*a*)). The point at which the atrium (which is part of the HT) ends and the OVs (which are not) begin is hard to discern. The presence of heartbeat is another complicating factor with the heart tube shortening during systole. Another significant difficulty is the nonplanar topology as a loop is formed (Fig. 2(*d*)).

In spite of these challenges, we proceeded with length measurements because we wanted to confirm results from almost 100 years ago [15] and because length is an important quantity. We used an indirect method to estimate heart tube length by tracing the outer curvature of hearts whose rotation has been eliminated (Sec. 2.5). We were conservative in our approach and used only those embryos in which the heart shape was perfectly planar and could be traced easily in ImageJ. Based on our results (Sec. 3.3), we get a growth stretch ratio of $\lambda_g = 1.49$ during early s-looping. These results are consistent with those in Ref. [15].

Since length is such a basic quantity and reliable measurements are hard, we obtained measurements from a third source: some of the clearest and most beautiful images of cardiac looping are found in the electron microscopy images in Ref. [1], which presents rotated ventral views in which the HT outer curvature can be traced. By doing so, we obtained a growth stretch ratio of 1.33 during early s-looping, based on images from HH 13 and HH 15 hearts. Based on these results, we conclude that the heart undergoes a 30–50% increase in length during early s-looping in the chick. A recent paper quantifies several aspects of mouse heart development during the looping phase, including length [22]. During the stages in mouse development that approximately correspond to the chick s-looping phase considered here, the growth stretch ratio for the mouse heart tube is in the range 1.27–1.90, which is consistent with the values reported above.

In our physical model, $\lambda_g = 1.31$ is able to generate a loop whose topology is the same as in experiment (Figs. 6(*d″*) and 2(*d*)). Cell proliferation likely accounts for the increase in length. A "caudal proliferating growth center" causes addition of cells to the venous pole. Some of these proliferating cells also migrate to the arterial pole [26].

It is obvious that a tube fixed at its ends and growing (or equivalently a tube of fixed length whose ends are brought together) will form a loop. The idea was considered by early studies [6]. These classical ideas were recently explained clearly using a physical model in Ref. [16], where the authors introduce the *growth induced buckling hypothesis*. Using a physical model, the authors are able to demonstrate that lengthening of the heart tube relative to lengthening of the pericardial cavity can lead to s-loop formation. However, a heart tube in which all the major segments lie on the same plane will not form a loop as it grows; it will form a hairpin bend (Figs. 2(*d′*), 6(*d′*), 8(*d*), and 8(*d′*)).

Some action is needed to displace one end of the heart tube into a different plane. According to Ref. [16], the factor forcing the elongating heart tube into an s-shaped configuration is the resistance of the wall of the pericardial cavity, i.e., growth within a physically confined space. And leftward displacement of the venous pole relative to the arterial pole is the cause for the normal bias toward D-loop handedness. In this study, we believe that rotation of the embryo, which starts from the cranial end and proceeds caudad, pushes the arterial pole of the heart tube into a different frontal plane, and sets the stage for loop formation. The idea was first put forth in Ref. [15] and is developed further in our study.

4.2 Remarks on Link Between Cardiac Looping and Embryonic Torsion. Early studies indicate that the purpose of torsion is to turn the embryo sideways so that the stiff bulk of

the yolk is no longer an impediment to flexion, which occurs simultaneously and leads to the transformation of the straight longitudinal embryonic axis to the familiar curved fetal position (Figs. 3(*a*)–3(*d*)). As a result of torsion, the embryo lies with its right lateral edge away from the yolk and the left lateral edge on it. Torsion is a gradual process and starts at the cranial end shortly after HH Stage 12 (48 h). It progresses caudad until the entire embryo is turned to its side. Torsion and flexion occur simultaneously and are highly correlated spatially and temporally [15,27]. According to our hypothesis (Sec. 4.4), a combination of heart tube elongation and cervical flexure provides the forces driving cardiac s-loop formation. Embryonic torsion ensures that these forces consistently form a loop.

Head torsion displaces the cranial end of the heart tube backward (i.e., away from the observer in Fig. 2). The cranial and caudal ends of the tube, which are now in different frontal planes, can form a loop when they are brought together by a combination of compressive forces due to HT elongation and cervical flexure (Figs. 2(*a*)–2(*d*), 6(*a*)–6(*d*), and 7(*a*)–7(*d*)). If head rotation is removed, the cranial end of the HT ends up in the same plane as the caudal end (Figs. 2(*a*′), (2*b*′), 6(*a*′), 6(*b*′), 8(*a*), and 8(*b*)). With this improper preloop, we expect the formation of a hairpin bend when the tube is acted on by forces due to HT elongation and cervical flexure. Our experiments and models confirm this intuitive idea: when torsion is impaired by hair-insertion, most hearts (68%) developed the hairpin bend. Our physical and computational models echo the dominant experimental result (Figs. 2(*b*′)–2(*d*′), 6(*b*′)–6(*d*′), and 8(*b*)–8(*d*)).

When torsion is inhibited, a minority of hearts (20%) formed loops (at varying levels of completion) on the left side of the embryo. The reasons behind this adaptation are not currently known, but it is tempting to speculate a role for Beloussov's hyper-restoration hypothesis [28]. According to this theory, embryonic tissues want to maintain a certain baseline stress state. When this state is perturbed, the tissue response overshoots the original state. It is possible that the shift to the left that we observed is an example of such overshoot. Heart loops on the left side are also known to occur as a result of other perturbations [17,29].

We also investigated the converse question: is it possible that cardiac torsion provides the driving torque and that head rotation follows as a result? Material testing has revealed that the shear modulus of the embryonic brain is about ten times bigger than that of the heart [18]. It is of course easier for a stronger material to twist a lighter one than vice versa. To investigate further, we removed hearts from stage 12 or 13 embryos where there is no rotation or rotation has barely started. Our results clearly indicate that head torsion can proceed as normal in the absence of cardiac forces (Sec. 3.2.2, Fig. 5), especially in embryos where some initial rotation is present. These results are in agreement with other studies where the heart was removed and rotation was observed [14]. However, Ref. [30] reports that, when hearts are removed from young embryos (stage 11 and lower), rotation is affected. We also found that in younger embryos head rotation (as well as cranial flexure) progressed less robustly (Sec. 3.2.2).

The mechanisms driving head torsion are currently not understood fully. Torsion always seems to be initiated cranially and proceeds caudad and embryonic membranes may play a role in driving torsion [31]. It is also known that disrupting body flexures does not inhibit rotation [32]. Interestingly, manually moving the heart to the left side induces leftward rotation [33].

4.3 Remarks on Link Between Cardiac Looping and Embryonic Flexures. There are two main flexures in the developing head and neck region: Cranial flexure, which causes the axes of the forebrain and the hindbrain to form a right angle (Figs. 1(*d*) and 5(*d*)) and cervical flexure, which forms a broad curve on the dorsal body wall (Figs. 1(*d*) and 4(*a*)). It is been showed that cranial flexure and heart looping are decoupled. Heart-free embryos are able to form normal cranial flexures [30] and disrupting cranial flexure does not impact heart looping [34]. Our results support these findings—embryos lacking a heart are able to form normal cranial flexures (Sec. 3.2.2, Fig. 5).

Cervical flexure occurs and deepens in the same developmental window as early s-looping (HH 13 to HH15/16). Männer established that with regards to cervical flexure and s-looping, the former is the cause and the latter is the effect. When cervical flexure is suppressed by inserting a human hair into the neural tube, a normal s-loop is not formed [32]. Prior studies had suggested that the looping heart pulls on the dorsal body wall, leading to cervical flexure and severing the heart tube resulted in the absence of flexure formation [13]. However, it was later shown that the loss of flexure in this case is due to lack of oxygen arising from loss of blood circulation; and that culturing heart-free embryos in an oxygen-rich environment (to compensate for oxygen loss due to absence of blood flow) normalizes flexure [14].

The results of this study support and extend this finding. The prior study used an angle measure to quantify curvature, whereas we measured the radius of curvature of the cervical flexure segment directly, whereas the prior study used the windowing method of culture and right lateral views, we used our filter-paper method (Sec. 2.1) with ventral and left lateral views. We measured the length of the cervical flexure segment by evaluating a numerical line integral (Sec. 2.4).

Using a different culture technique and a different method to quantify curvature, we arrived at the same result: cervical flexure can form in the absence of cardiac forces. And since we tracked length, we are able to look at flexure formation more closely. Although the radius of the cervical flexure arc decreased in both control and heart-free embryos (a smaller radius indicates a more curved structure), we found that the length of the cervical flexure arc did not increase robustly in heart-free embryos compared to control embryos; similar effects were reported in the previous study [14]. It is possible that the effect of eliminating circulation via heart removal is not fully compensated by incubating in an oxygen-rich environment.

However, our essential conclusion is the same as in Ref. [14]: cervical flexure can form in the absence of cardiac forces. Indeed, there is no statistical difference in normalized curvatures between control and heart-removed embryos (0.63 for controls and 0.68 for heart-free embryos, respectively—Sec. 3.2.1). It is interesting to note that a very similar ratio, 0.65, is obtained for the physical model (Sec. 3.4) for an initial loop (Fig. 6(*c*)). The value obtained for a full loop (Fig. 6(*d*), ratio = 0.41), is smaller likely because the physical model in Figs. 6(*a*)–6(*d*) does not include heart tube growth. Hence, it is not surprising that more flexure (i.e., smaller radius) is needed to produce looping of the heart tube in the model. And the smaller radius leads to a smaller ratio. But it is also important to note here the many differences between the physical model and experiment (Sec. 2.6).

The distance between the arterial and venous poles was not quantified in our study, but it is known that a shortening of this distance is an essential characteristic of s-looping in the chick [1,7]. And pole convergence is likely caused by cervical flexure [32]. The distance between the poles for the developing mouse heart is considered in Ref. [22].

Developmental anomalies of the head and neck often involve congenital cardiovascular defects (e.g., septal defects) and impaired brain function (e.g., intellectual impairment). An example is the CHARGE association, which involves developmental anomalies of the eye, ear, heart, and brain. Another example is the 22q11.2 Deletion Syndrome, which has an estimated incidence of 1 out of 4000 live births and is present in 1 out of 68 children with congenital heart disease ([35] and references therein). Please note that even though our results show that cervical flexure and heart development are crucially linked, currently no evidence exists directly linking improper cervical flexure to the disorders mentioned above. It is, however, known that altered flexion can lead to delayed closure of the posterior neuropore [36]. And accelerated and delayed body flexion can lead to polysplenia and asplenia [37].

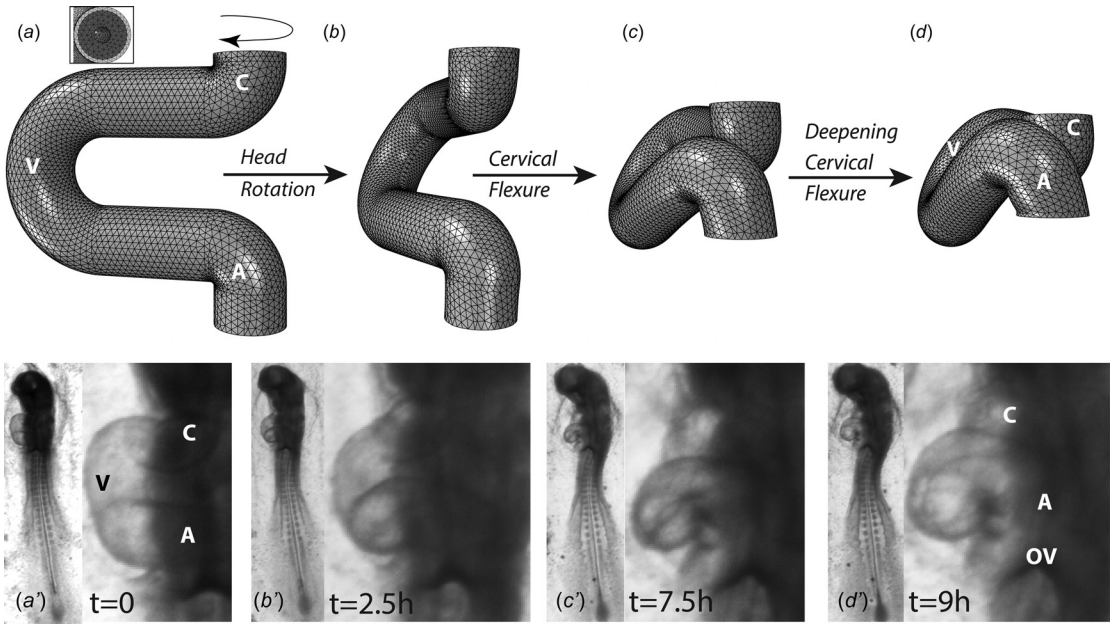

Fig. 7 Finite element model of early cardiac s-looping in control conditions. Top row shows time progression of model while bottom row shows the experiment at comparable time points (whole embryo pictures are shown along with heart close-ups). ((*a*), (*a*′)) heart at $t = 0$ that is not rotated. Inset in model shows cross section where a thin layer of myocardium encloses a thicker layer of cardiac jelly (extracellular matrix) which in turn encloses a circular lumen. Curved arrow at top end shows the direction of head rotation. ((*b*), (*b*′)) heart when head rotation is completed. ((*c*), (*d*) and (*c*′), (*d*′)) gradual progression of cervical flexure brings together the conotruncus and the atrium and completes the loop. (V = ventricle, A = atrium, C = conotruncus (outflow tract, arterial pole), and OV = omphalomesenteric veins, (inflow, venous pole)).

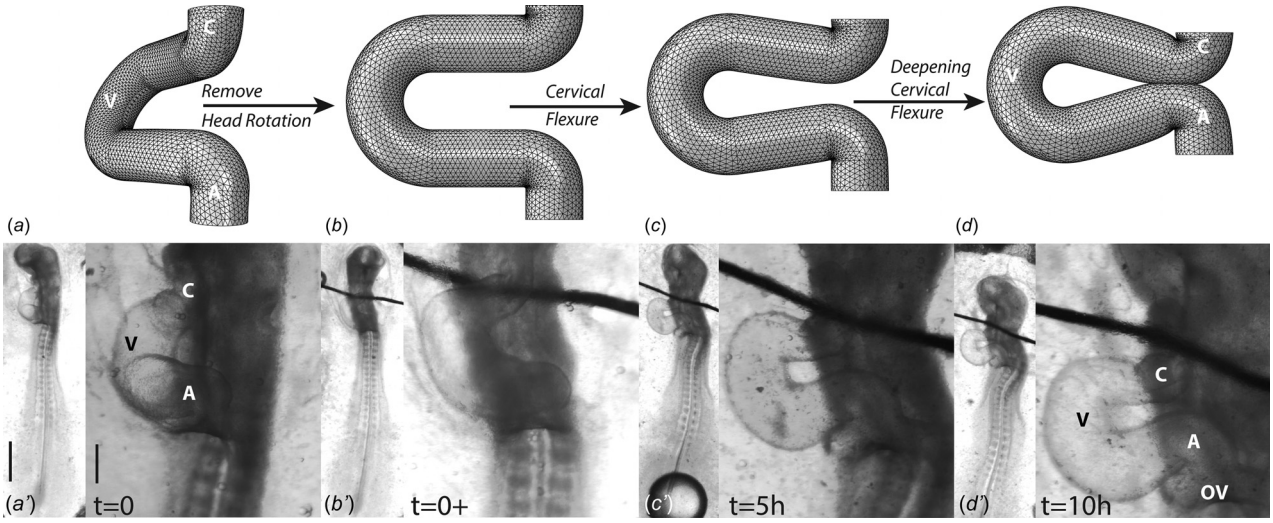

Fig. 8 Finite element model of early cardiac s-looping when torsion is inhibited. Top row shows the time progression of the model while the bottom row shows the experiment at comparable time points (whole embryo pictures are shown along with heart close-ups). ((*a*), (*a*′)) Heart in embryo that has undergone torsion, but not flexure. ((*b*), (*b*′)) Heart configuration when head rotation has been removed (note inserted hair in experiment; rotational loads are removed in model). ((*c*), (*c*′) and (*d*), (*d*′)) Heart configuration when flexure is allowed to continue in the absence of torsion. Note the formation of the "hairpin bend" configuration in (*d*) and (*d*′). In this particular embryo, the conotruncus and the atrium do not touch each other at $t = 10$ h ((*d*′)), but they do in other embryos (please see Fig. 2(*d*′)). (V = ventricle, A = atrium, C = conotruncus (outflow tract, arterial pole), and OV = omphalomesenteric veins, (inflow, venous pole)). Scale bar in whole embryo pictures = 1 mm. Scale bar in heart close-ups = 250 μm.

We noted regrowth when the heart was cut away. This was particularly significant at the caudal attachment point (Fig. 3(*d*′)). This is not surprising given the importance of the caudal regions in proliferation [26].

4.4 An Improved Hypothesis for Early S-Looping. Our experiments and models show that s-loop formation is composed of two actions: in action 1, the cranial and caudal portions of the heart tube, which are more or less in the same plane following the

completion of c-looping, are twisted into different planes. In action 2, compressive forces transform the twisted c-loop into an s-loop (Figs. 2(*a*)–2(*d*), 6(*a*)–6(*d*), and 7(*a*)–7(*d*)).

Several forces act in concert to ensure that a proper twist is achieved in action 1. The downward pressure applied by the SPL has the effect of displacing the cranial portion of the heart tube into a different plane [12] and the larger left omphalomesenteric vein also causes a twist during c-looping [10,20]. However, data in this study indicate that a significant source of twist comes from the rotation of the head to the right (Figs. 5(*a*)–5(*c*), 6(*a*), 6(*b*), 7(*a*), and 7(*b*)). That the twist is a strong force is apparent when it is removed. There is dramatic loss of three-dimensional structure and the heart reverts to a planar c-loop (Figs. 2(*a*′), 2(*b*′), 2(*a*″), 2(*b*″), 6(*b*′), 8(*a*), and 8(*b*)). Prolonged culture in the presence of impaired rotation leads to a planar hairpin bend configuration (Figs. 2(*d*′), 6(*d*′), 8(*d*), and 8(*d*′)). Experiments in mouse embryos also indicate a rotation of the arterial pole of the heart tube [22]. This paper also provides measurements of the extent to which rotation occurs during looping.

Multiple forces act in concert to ensure that proper compression is applied (action 2). In 2013, we presented a hypothesis for early s-looping, the first of its kind. In this hypothesis, we postulated that cervical flexure provides the necessary force to convert the twisted c-loop into an s-loop. Cervical flexure is indeed important and preventing it certainly arrests the complete formation of an s-loop [32].

However, we noted that embryos with nearly same cervical flexure radius can have vastly different looping morphologies. By considering these differences in looping morphology when cervical flexure is constant, we independently arrived at the same conclusion as in Ref. [16], i.e., rapid increase in heart tube length relative to the length of the pericardial cavity provides an additional compressive force that aids in s-loop formation. Our physical model shows that growth in the heart tube can indeed produce an s-loop (Figs. 6(*a*″)–6(*d*″)). We can now improve the hypothesis for s-loop formation that was presented in Ref. [12].

Action 1: Following c-looping, the following forces ensure that the cranial portion of the heart tube is displaced (i.e., away from the observer in a left lateral view) compared to the caudal portion (experiment: Figs. 5(*a*)–5(*c*), model: Figs. 6(*a*) and 6(*b*) and 7(*a*) and 7(*b*)): (1) torsion provided by head rotation, (2) increased growth in the left omphalomesenteric vein, and (3) downward pressure from the splanchnopleure.

Action 2: Concurrently, the following forces ensure that a compressive force is applied to the ends of the heart tube: (1) the formation and deepening of cervical flexure and (2) rapid growth of the heart tube. These result in shortening of the distance between the conotruncus and the common atrium leading to loop formation. (Experiment: Figs. 2(*a*)–2(*c*); model: Figs. 6(*b*), 6(*c*), 7(*b*), and 7(*c*) when cervical flexure provides the compressive force and Figs. 6(*b*″) and 6(*c*″) when growth provides the compressive force.)

Outcome: Continued application of these two concurrent actions results in a three-dimensional loop where the ventricle moves inferior to the common atrium (experiment: Fig. 2(*d*); model: Figs. 6(*d*), 6(*d*″), and 7(*d*)).

5 Limitations

The following are the limitations in our study: (1) although quantitative measurements are provided for progression of cervical flexure and length of the heart tube, the observations on embryonic torsion and cranial flexure are qualitative in nature. (2) The perturbation studies described here only block gross shape changes like flexion and torsion. The underlying cellular and molecular mechanisms could still be active. (3) Embryonic flexure and torsion are tightly coupled temporally and spatially; but our experiments inhibiting torsion do not consider the effect on flexures. (4) We have not precisely quantified the various normal and abnormal loop morphologies (the mathematical discipline of topology would be immensely helpful here). (5) The initial finite element model geometry is simple and tubular and does not exactly match the experimental heart shape (compare Figs. 7(*a*) and 7(*a*′)). Because of this, there are small differences between the loop topologies formed by the model and the experiment. For instance, the portions of the conus in the model are displaced caudal to portions of the atrium, a situation not present in the experiment (compare Figs. 7(*d*) and 7(*d*′)).

Acknowledgment

We thank Dr. Larry Taber, Kaelan Hansson, and Dima Yankova for their help. We also thank Dr. Roger Hoerl for assistance with statistical analysis. The authors also wish to thank technicians Mark Hooker and Stan Gorski for their help with the physical model.

Funding Data

- National Heart, Lung, and Blood Institute (Grant No. R15HL110009; Funder ID: 10.13039/100000050).
- Union College Summer Fellowship Program (Funder ID: 10.13039/100007193).
- Union College Faculty Research Fund (Funder ID: 10.13039/100007193).
- National Science Foundation (Grant No. NSF DUE 0850242; Funder ID: 10.13039/501100008982).

References

[1] Manner, J., 2000, "Cardiac Looping in the Chick Embryo: A Morphological Review With Special Reference to Terminological and Biomechanical Aspects of the Looping Process," Anat. Rec., **259**, pp. 248–262.

[2] Manner, J., Wessel, A., and Yelbuz, T. M., 2010, "How Does the Tubular Embryonic Heart Work? Looking for the Physical Mechanism Generating Unidirectional Blood Flow in the Valveless Embryonic Heart Tube," Dev. Dyn., **239**, pp. 1035–1046.

[3] Taber, L. A., 2006, "Biophysical Mechanisms of Cardiac Looping," Int. J. Dev. Biol., **50**(2–3), pp. 323–332.

[4] Sylva, M., van den Hoff, M. J., and Moorman, A. F., 2014, "Development of the Human Heart," Am. J. Med. Genet., Part A, **164**(6), pp. 1347–1371.

[5] Hamburger, V., and Hamilton, H. L., 1951, "A Series of Normal Stages in the Development of the Chick Embryo," J. Morphol., **88**(1), pp. 49–92.

[6] Bremer, J. L., 1928, "Experiments on the Aortic Arches in the Chick," Anat. Rec., **37**(3), pp. 225–254.

[7] Manner, J., 2004, "On Rotation, Torsion, Lateralization, and Handedness of the Embryonic Heart Loop: New Insights From a Simulation Model for the Heart Loop of Chick Embryos," Anat. Rec., **278**(1), pp. 481–492.

[8] Manner, J., 2013, "On the Form Problem of Embryonic Heart Loops, Its Geometrical Solutions, and a New Biophysical Concept of Cardiac Looping," Ann. Anat., **195**(4), pp. 312–323.

[9] Ramasubramanian, A., Latacha, K. S., Benjamin, J. M., Voronov, D. A., Ravi, A., and Taber, L. A., 2006, "Computational Model for Early Cardiac Looping," Ann. Biomed. Eng., **34**(8), pp. 1655–1669.

[10] Ramasubramanian, A., Nerurkar, N., Achtien, K., Filas, B., Voronov, D., and Taber, L., 2008, "On Modeling Morphogenesis of the Looping Heart Following Mechanical Perturbations," ASME J. Biomech. Eng., **130**(6), p. 061018.

[11] Shi, Y., Yao, J., Young, J. M., Fee, J. A., Perucchio, R., and Taber, L. A., 2014, "Bending and Twisting the Embryonic Heart: A Computational Model for c-Looping Based on Realistic Geometry," Front. Physiol., **5**, p. 297.

[12] Ramasubramanian, A., Chu-Lagraff, Q., Buma, T., Chico, K., Carnes, M., Burnett, K., Bradner, S., and Gordon, S., 2013, "On the Role of Intrinsic and Extrinsic Forces in Early Cardiac s-Looping," Dev. Dyn., **242**(7), pp. 801–816.

[13] Flynn, M. E., Pikalow, A. S., Kimmelman, R. S., and Searls, R. L., 1991, "The Mechanism of Cervical Flexure Formation in the Chick," Anat. Embryol., **184**(4), pp. 411–420.

[14] Männer, J., Seidl, W., and Steding, G., 1995, "Formation of the Cervical Flexure: An Experimental Study on Chick Embryos," Acta Anat., **152**(1), pp. 1–10.

[15] Patten, B. M., 1922, "The Formation of the Cardiac Loop in the Chick," Am. J. Anat., **30**(3), pp. 373–397.

[16] Bayraktar, M., and Manner, J., 2014, "Cardiac Looping May Be Driven by Compressive Loads Resulting From Unequal Growth of the Heart and Pericardial Cavity. Observations on a Physical Simulation Model," Front. Physiol., **5**, p. 112.

[17] Voronov, D. A., and Taber, L. A., 2002, "Cardiac Looping in Experimental Conditions: Effects of Extraembryonic Forces," Dev. Dyn., **224**(4), pp. 413–421.

[18] Xu, G., Kemp, P. S., Hwu, J. A., Beagley, A. M., Bayly, P. V., and Taber, L. A., 2010, "Opening Angles and Material Properties of the Early Embryonic Chick Brain," ASME J. Biomech. Eng., **132**(1), p. 011005.
[19] Zamir, E. A., and Taber, L. A., 2004, "Mechanical Properties and Residual Stress in the Stage 12 Chick Heart During Cardiac Looping," ASME J. Biomech. Eng., **126**(6), pp. 823–830.
[20] Voronov, D. A., Alford, P. W., Xu, G., and Taber, L. A., 2004, "The Role of Mechanical Forces in Dextral Rotation During Cardiac Looping in the Chick Embryo," Dev. Biol., **272**(2), pp. 339–350.
[21] Latacha, K. S., Remond, M. C., Ramasubramanian, A., Chen, A. Y., Elson, E. L., and Taber, L. A., 2005, "Role of Actin Polymerization in Bending of the Early Heart Tube," Dev. Dyn., **233**(4), pp. 1272–1286.
[22] Le Garrec, J.-F., Domínguez, J. N., Desgrange, A., Ivanovitch, K. D., Raphaël, E., Bangham, J. A., Torres, M., Coen, E., Mohun, T. J., and Meilhac, S. M., 2017, "A Predictive Model of Asymmetric Morphogenesis From 3D Reconstructions of Mouse Heart Looping Dynamics," eLife, **6**, p. e28951.
[23] Drake, C. J., Wessels, A., Trusk, T., and Little, C. D., 2006, "Elevated Vascular Endothelial Cell Growth Factor Affects Mesocardial Morphogenesis and Inhibits Normal Heart Bending," Dev. Dyn., **235**(1), pp. 10–18.
[24] Harvey, R. P., 1998, "Cardiac Looping—An Uneasy Deal With Laterality," Semin. Cell Dev. Biol., **9**(1), pp. 101–108.
[25] Srivastava, D., and Olson, E. N., 1997, "Knowing in Your Heart What's Right," Trends Cell Biol., **7**(11), pp. 447–453.
[26] van den Berg, G., Abu-Issa, R., de Boer, B. A., Hutson, M. R., de Boer, P. A., Soufan, A. T., Ruijter, J. M., Kirby, M. L., van den Hoff, M. J., and Moorman, A. F., 2009, "A Caudal Proliferating Growth Center Contributes to Both Poles of the Forming Heart Tube," Circ. Res., **104**(2), pp. 179–188.
[27] Patten, B. M., 1951, *Early Embryology of the Chick*, 4th ed., McGraw-Hill, New York.
[28] Beloussov, L. V., 1998, *The Dynamic Architecture of a Developing Organism: An Interdisciplinary Approach to the Development of Organisms*, Springer, Dordrecht, The Netherlands.
[29] Hoyle, C., Brown, N. A., and Wolpert, L., 1992, "Development of Left/Right Handedness in the Chick Heart," Development, **115**(4), pp. 1071–1078.
[30] Waddington, C. H., 1937, "The Dependence of Head Curvature on the Development of the Heart in the Chick Embryo," J. Exp. Biol., **14**, pp. 229–231.
[31] Deuchar, E. M., 1971, "The Mechanism of Axial Rotation in the Rat Embryo: An Experimental Study In Vitro," J. Embryol. Exp. Morphol., **25**(2), pp. 189–201.
[32] Männer, J., Seidl, W., and Steding, G., 1993, "Correlation Between the Embryonic Head Flexures and Cardiac Development: An Experimental Study in Chick Embryos," Anat. Embryol., **188**, pp. 269–285.
[33] Chen, Z., Guo, Q., Dai, E., Forsch, N., and Taber, L. A., 2017, "How the Embryonic Chick Brain Twists," J. R. Soc., Interface, **13**(124), p. 20160395.
[34] Manner, J., Seidl, W., and Steding, G., 1995, "The Role of Extracardiac Factors in Normal and Abnormal Development of the Chick Embryo Heart: Cranial Flexure and Ventral Thoracic Wall," Anat. Embryol., **191**, pp. 61–72.
[35] Wenger, T. L., McDonald-McGinn, D. M., and Zackai, E. H., 2014, "Genetics of Common Congenital Syndromes of the Head and Neck," *Congenital Malformations of the Head and Neck*, Springer, New York, pp. 1–22.
[36] van Straaten, H., Hekking, J., Consten, C., and Copp, A., 1993, "Intrinsic and Extrinsic Factors in the Mechanism of Neurulation: Effect of Curvature of the Body Axis on Closure of the Posterior Neuropore," Development, **117**(3), pp. 1163–1172.
[37] Hutchins, G., Moore, G., Lipford, E., Haupt, H. M., and Walker, M. C., 1983, "Asplenia and Polysplenia Malformation Complexes Explained by Abnormal Embryonic Body Curvature," Pathol., Res. Pract., **177**(1), pp. 60–76.